



Optimal field-free orientation of molecules with resonant tailored multicolor fields

Zhang, Jin Ping; Wang, Shuo; Henriksen, Niels E.

Published in:
Physical Review A

Link to article, DOI:
[10.1103/PhysRevA.107.033118](https://doi.org/10.1103/PhysRevA.107.033118)

Publication date:
2023

Document Version
Publisher's PDF, also known as Version of record

[Link back to DTU Orbit](#)

Citation (APA):
Zhang, J. P., Wang, S., & Henriksen, N. E. (2023). Optimal field-free orientation of molecules with resonant tailored multicolor fields. *Physical Review A*, 107(3), Article 033118.
<https://doi.org/10.1103/PhysRevA.107.033118>


General rights

Copyright and moral rights for the publications made accessible in the public portal are retained by the authors and/or other copyright owners and it is a condition of accessing publications that users recognise and abide by the legal requirements associated with these rights.

- Users may download and print one copy of any publication from the public portal for the purpose of private study or research.
- You may not further distribute the material or use it for any profit-making activity or commercial gain
- You may freely distribute the URL identifying the publication in the public portal

If you believe that this document breaches copyright please contact us providing details, and we will remove access to the work immediately and investigate your claim.

Optimal field-free orientation of molecules with resonant tailored multicolor fields

Jin-Ping Zhang and Shuo Wang ^{*}*School of Physics, Dalian University of Technology, Dalian 116024, People Republic of China*Niels E. Henriksen *Department of Chemistry, Technical University of Denmark, Building 206, DK-2800 Kongens Lyngby, Denmark*

(Received 13 September 2022; revised 5 January 2023; accepted 14 March 2023; published 29 March 2023)

Optimal field-free molecular orientation for a given number of populated states, achieved by using resonant laser pulses, is theoretically investigated for linear molecules. An optimal phase difference between the rotational states can be obtained, at full revival times, after the laser pulses have decayed and these phase conditions are analytically derived for multilevel systems ($J > 2$). The dependence of the phase difference on the duration and absolute area of the laser pulses is analyzed. Finally, the optimal degree of molecular orientation can be obtained by adjusting the ratios of the peak amplitudes of the laser pulses, with the carrier-envelope phases or the delay time between the pulses fulfilling the phase conditions.

DOI: [10.1103/PhysRevA.107.033118](https://doi.org/10.1103/PhysRevA.107.033118)

I. INTRODUCTION

Molecular alignment and orientation have long been noted for playing a critical role in many physical and chemical processes, such as controlling the probability of ionization and chemical reaction control [1–7]. Spatially aligned and oriented molecules can also be viewed as crucial prerequisites for high-order harmonic generation [8–10], which is widely used in molecular imaging [11], nuclear dynamics retrieving [12], and attosecond pulse production [13].

Molecular alignment has been well studied both theoretically and experimentally [6,14–16]. As a head-versus-tail order of the molecules needs to be established, controlling molecular orientation is more challenging. Many theoretical and experimental studies have been carried out to control molecular orientation, see Ref. [17] (and references therein), which can be roughly divided into adiabatic and nonadiabatic schemes. When the pulse duration τ is sufficiently longer than molecular rotational periods T_{rot} , i.e., $\tau \gg T_{\text{rot}}$, molecules are adiabatically oriented in laser fields. The adiabatic orientation is obtained by using laser pulses with long temporal widths, and a high degree of orientation can be obtained with the help of optimal phase differences between adjacent rotational states at full revival times [18–22].

For the case of $\tau \ll T_{\text{rot}}$, molecules are nonadiabatically oriented after the laser pulse. One regime is based on the interaction between ultrashort nonresonant two-color laser pulses and the molecular hyperpolarizability, which can change the parity of the wave function [23–26]. Alternatively, laser fields in the THz region have been used to control molecular orientation by permanent dipole-moment interaction. In the sudden-impact limit, half-cycle THz laser pulses (HCP) and few-cycle THz pulses [27,28], with asymmetric temporal

waveforms, are utilized to excite many rotational states based on the “kick” mechanism [29–31], while time-symmetric single-cycle pulses [32–35] with pulse duration comparable to the rotational period of molecules are used to induce resonant dipole transitions between neighboring rotational states. In addition, some combination schemes were proposed in order to excite higher rotational states for a high degree of orientation [36–38]. It is necessary to ensure that the frequency spectrum of the laser pulses overlap with the rotational energy differences. Another key point is to get an optimal phase difference between adjacent populated rotational states at full revival times, independent of the rotational state, which is challenging for a nonadiabatic process [39,40].

Recent works show that, in the nonadiabatic limit, an optimal degree of alignment or orientation is obtained when an optimal phase difference appears at full revival times [33,41]. Furthermore, the phase differences can be well controlled in a three-state system according to the analytically derived optimal amplitude and phase conditions [42]. As the upper limit for the degree of orientation in a three-state system is 0.775 [22], it is highly desirable to consider the case including more rotational states. However, it is challenging to give an analytical description for multilevel systems ($J > 2$).

In this paper, we use a set of resonant laser pulses to control the molecular orientation. The phase conditions for multilevel systems ($J > 2$) are analytically derived based on the first-order Magnus expansion. According to the analytical description, an optimal phase difference can be obtained at full revival times by a simple choice of the carrier-envelope phases of the laser pulses. Furthermore, the dependence of the dynamics of the system on the absolute area of the laser pulses is discussed. It shows that the absolute area of the pulses has to be controlled to satisfy the phase condition. Finally, an optimal orientation can be obtained by adjusting the ratio of the laser pulse intensities when the phase conditions are satisfied.

^{*}wangshuo@dlut.edu.cn

II. THEORY

A. Model and basic equations

In our scheme, linearly polarized resonant laser pulses are used to control the field-free orientation of a linear molecule. The form of the laser pulses is expressed as a superposition of Gaussian pulses

$$E(t) = \sum_{J=1} \varepsilon_J \exp\left(-4 \ln 2 \frac{(t-t_J)^2}{\tau^2}\right) \times \cos[\omega_{J,J-1}(t-t_J) + \phi_J] \quad (J=1, 2, 3, \dots), \quad (1)$$

where ε_J , t_J , and ϕ_J are the electric-field amplitude, center time, and carrier-envelope phase of the J th laser pulse, respectively, $\omega_{J,J-1}$ is the transition frequencies of the rotational states, and τ is the full width at half maximum (FWHM). Within the rigid-rotor approximation, the Hamiltonian of the molecule irradiated by laser pulses is given by $\hat{H}(t) = \hat{H}_0 + \hat{V}(t)$, with the field-free Hamiltonian $\hat{H}_0 = B\hat{J}^2$ and the dipole interaction term $\hat{V}(t) = -\mu E(t) \cos \theta$. B is the rotational constant, \hat{J} is the angular-momentum operator, μ is the permanent dipole moment, and θ is the angle between laser polarization and the molecular axis.

The dynamics are formulated in terms of the density-matrix method. The time evolution of the density operator is determined by the quantum Liouville equation, which can be solved by using the fourth-order Runge–Kutta method [43]. In the $|JM\rangle$ state representation, the degree of molecular orientation after the laser pulses have decayed is given by ($\hbar = 1$)

$$\begin{aligned} \langle \cos \theta \rangle(t) &= 2 \sum_{J=0}^{J_{\max}} \sum_{M=-J}^J |C_{J,M} C_{J-1,M}| \\ &\times \langle J, M | \cos \theta | J-1, M \rangle \\ &\times \cos(\Delta E_{J,J-1} t - \varphi_{J,J-1}), \end{aligned} \quad (2)$$

where J_{\max} is the highest rotational state in the sum, $C_{J,M}$ is the complex coefficient of the rotational state, $\Delta E_{J,J-1} = 2BJ$, and $\varphi_{J,J-1} = \arg(C_{J,M}) - \arg(C_{J-1,M})$ are energy differences

and constant phase differences between adjacent rotational states, respectively. The full revivals in the field-free orientation occur at a time interval $T_{\text{rot}} = \pi/B$ and maximal orientation for a given coherent superposition of states is obtained when the phase difference between adjacent rotational states $\Delta E_{J,J-1} t - \varphi_{J,J-1}$ equals $2k\pi$ or $(2k+1)\pi$, where $k = 0, \pm 1, \pm 2, \dots$. We can get the full revival time t_{rev} from $\Delta E_{1,0} t_{\text{rev}} - \varphi_{1,0} = 2B t_{\text{rev}} - \varphi_{1,0} = 2k\pi$ or $(2k+1)\pi$. Then we substitute t_{rev} into $\Delta E_{J,J-1} t_{\text{rev}} - \varphi_{J,J-1} = 2BJ t_{\text{rev}} - \varphi_{J,J-1} = 2k\pi$ or $(2k+1)\pi$ and obtain the phase conditions as follows:

$$\begin{aligned} \varphi_{J,J-1} - J\varphi_{1,0} &= 2k\pi, \\ \text{or } \varphi_{J,J-1} - J\varphi_{1,0} &= (J-1)(2k+1)\pi, \quad (k=0, \pm 1, \pm 2, \dots). \end{aligned} \quad (3)$$

When the phase conditions are satisfied, the phase differences between adjacent rotational states are in phase at the full revival times $t_{\text{rev}} = (2k\pi + \varphi_{1,0})/2B$ or $[(2k+1)\pi + \varphi_{1,0}]/2B$.

B. The phase conditions for a multilevel system

To derive the dependence of phase conditions in Eq. (3) on the laser pulses, we extend the derivation in Refs. [33,42] to a multilevel system and discuss the underlying physics. The theoretical derivation is based on the first-order Magnus expansion. The time evolution of the system in the interaction picture, from the initial time t_0 to a given time t , can be described by the unitary operator

$$\hat{U}(t, t_0) = \mathbb{I} - i \int_{t_0}^t \hat{H}_I(t') \hat{U}(t', t_0) dt', \quad (4)$$

where $\hat{H}_I(t) = \exp(i\hat{H}_0 t) \hat{V}(t) \exp(-i\hat{H}_0 t)$ is the Hamiltonian in the interaction picture. The matrix element of $\hat{H}_I(t)$ in the $|JM\rangle$ state representation is $-\mu_{J',J} E(t) \exp(i\omega_{J',J} t)$ with $\mu_{J',J} = \mu \langle J', M | \cos \theta | J, M \rangle$ and $\omega_{J',J} = E_{J'} - E_J$.

Next, the Magnus expansion is performed on the time-evolution operator $\hat{U}(t, t_0) = \exp[\sum_{n=1}^{\infty} \hat{S}^{(n)}(t)]$ [42]. The first leading term is given by $\hat{S}^{(1)}(t) = iA(t) = -i \int_{t_0}^t dt' \hat{H}_I(t')$. In the $|JM\rangle$ state representation,

$$A(t) = \begin{pmatrix} 0 & \beta_{10}(t) & 0 & \cdots & 0 & 0 \\ \beta_{10}^*(t) & 0 & \beta_{21}(t) & \cdots & 0 & 0 \\ 0 & \beta_{21}^*(t) & 0 & \cdots & 0 & 0 \\ \vdots & \vdots & \vdots & \ddots & \vdots & \vdots \\ 0 & 0 & 0 & \cdots & 0 & \beta_{m,m-1}(t) \\ 0 & 0 & 0 & \cdots & \beta_{m,m-1}^*(t) & 0 \end{pmatrix}, \quad (5)$$

where

$$\beta_{m,m-1}(t) = \mu_{m,m-1} \int_{t_0}^t E(t') e^{-i\omega_{m,m-1} t'} dt'. \quad (6)$$

The unitary operator including the first-order term $\hat{S}^{(1)}(t)$ reads $\hat{U}^{(1)}(t, t_0) = \exp[iA(t)] = \sum_m \exp(i\lambda_m) |\lambda_m\rangle \langle \lambda_m|$, where λ_m is an eigenvalue of $A(t)$ and the corresponding eigenstate is $|\lambda_m\rangle$. Since $A(t)$ is a Hermitian matrix, λ_m is a real number. If the order of the matrix $A(t)$ is an odd number, one of the eigenvalues of $A(t)$ is zero. The other roots come in pairs, and the roots of each pair are opposite numbers for each other. For example, $\lambda_0 = 0$, $\lambda_1 = -\lambda_2$, $\lambda_3 = -\lambda_4$, \dots . If the order of the matrix $A(t)$ is an even number, the roots come in pairs, and the roots of each pair are opposite numbers of each other. In our scheme, the initial state is set to $|00\rangle$. Because the electric field of the pulse is linearly polarized, the quantum number M is conserved. The

eigenstate $|\lambda_k\rangle$ can be expanded in the $|JM\rangle$ state representation,

$$|\lambda_k\rangle = c_0^{(k)}|00\rangle + c_1^{(k)}|10\rangle + \cdots + c_m^{(k)}|m0\rangle. \quad (7)$$

The relationship between the complex coefficients in Eq. (7) can be obtained from the secular equation $A(t)|\lambda_k\rangle = \lambda_k|\lambda_k\rangle$. Then we have

$$\begin{aligned} c_1^{(k)} &= \frac{\lambda_k}{\beta_{10}} c_0^{(k)}, \\ c_2^{(k)} &= \frac{(\lambda_k^2 - |\beta_{10}|^2)}{\beta_{10}\beta_{21}} c_0^{(k)}, \\ c_3^{(k)} &= \frac{\lambda_k(\lambda_k^2 - |\beta_{10}|^2 - |\beta_{21}|^2)}{\beta_{10}\beta_{21}\beta_{32}} c_0^{(k)}, \\ c_4^{(k)} &= \frac{\lambda_k^4 - \lambda_k^2(|\beta_{10}|^2 + |\beta_{21}|^2 + |\beta_{32}|^2) + |\beta_{10}|^2|\beta_{32}|^2}{\beta_{10}\beta_{21}\beta_{32}\beta_{43}} c_0^{(k)}, \\ &\vdots \end{aligned} \quad (8)$$

The wave function after the laser pulses have decayed is given by

$$\begin{aligned} |\psi\rangle &= \hat{U}^{(1)}(t, t_0)|00\rangle = \sum_m e^{i\lambda_m t} |\lambda_m\rangle \langle \lambda_m | 00\rangle = (c_0^{(0)})^* e^{i\lambda_0 t} (c_0^{(0)}|00\rangle \\ &\quad + c_1^{(0)}|10\rangle + \cdots + c_m^{(0)}|m0\rangle) + (c_0^{(1)})^* e^{i\lambda_1 t} (c_0^{(1)}|00\rangle + c_1^{(1)}|10\rangle + \cdots + c_m^{(1)}|m0\rangle) + \cdots \\ &\quad + (c_0^{(m)})^* e^{i\lambda_m t} (c_0^{(m)}|00\rangle + c_1^{(m)}|10\rangle + \cdots + c_m^{(m)}|m0\rangle). \end{aligned} \quad (9)$$

By the substitution of Eq. (8) into Eq. (9), considering the relationship between the eigenvalues of $A(t)$ ($\lambda_1 = -\lambda_2$, $\lambda_3 = -\lambda_4$, ...), then we have $|\psi\rangle = C_0|00\rangle + C_1|10\rangle + \cdots + C_m|m0\rangle$, where

$$\begin{aligned} C_0 &= \left\{ |c_0^{(0)}|^2 + 2|c_0^{(1)}|^2 \cos \lambda_1 + 2|c_0^{(3)}|^2 \cos \lambda_3 + 2|c_0^{(5)}|^2 \cos \lambda_5 + \cdots + 2|c_0^{(m-1)}|^2 \cos \lambda_{m-1} \right\}, \\ C_1 &= \frac{i}{\beta_{10}} \left\{ 2\lambda_1 \sin \lambda_1 |c_0^{(1)}|^2 + 2\lambda_3 \sin \lambda_3 |c_0^{(3)}|^2 + \cdots + 2\lambda_{m-1} \sin \lambda_{m-1} |c_0^{(m-1)}|^2 \right\}, \\ C_2 &= \frac{1}{\beta_{10}\beta_{21}} \left\{ -|\beta_{10}|^2 |c_0^{(0)}|^2 + 2(\lambda_1^2 - |\beta_{10}|^2) \cos \lambda_1 |c_0^{(1)}|^2 + 2(\lambda_3^2 - |\beta_{10}|^2) \cos \lambda_3 |c_0^{(3)}|^2 \right. \\ &\quad \left. + \cdots + 2(\lambda_{m-1}^2 - |\beta_{10}|^2) \cos \lambda_{m-1} |c_0^{(m-1)}|^2 \right\}, \\ C_3 &= \frac{i}{\beta_{10}\beta_{21}\beta_{32}} \left\{ 2\lambda_1(\lambda_1^2 - |\beta_{10}|^2 - |\beta_{21}|^2) \sin \lambda_1 |c_0^{(1)}|^2 + 2\lambda_3(\lambda_3^2 - |\beta_{10}|^2 - |\beta_{21}|^2) \sin \lambda_3 |c_0^{(3)}|^2 \right. \\ &\quad \left. + \cdots + 2\lambda_{m-1}(\lambda_{m-1}^2 - |\beta_{10}|^2 - |\beta_{21}|^2) \sin \lambda_{m-1} |c_0^{(m-1)}|^2 \right\}, \\ C_4 &= \frac{1}{\beta_{10}\beta_{21}\beta_{32}\beta_{43}} \left\{ |\beta_{10}|^2 |\beta_{32}|^2 |c_0^{(0)}|^2 + 2[\lambda_1^4 - \lambda_1^2(|\beta_{10}|^2 + |\beta_{21}|^2 + |\beta_{32}|^2) + |\beta_{10}|^2 |\beta_{32}|^2] \cos \lambda_1 |c_0^{(1)}|^2 \right. \\ &\quad \left. + 2[\lambda_3^4 - \lambda_3^2(|\beta_{10}|^2 + |\beta_{21}|^2 + |\beta_{32}|^2) + |\beta_{10}|^2 |\beta_{32}|^2] \cos \lambda_3 |c_0^{(3)}|^2 \right. \\ &\quad \left. + \cdots + 2[\lambda_{m-1}^4 - \lambda_{m-1}^2(|\beta_{10}|^2 + |\beta_{21}|^2 + |\beta_{32}|^2) + |\beta_{10}|^2 |\beta_{32}|^2] \cos \lambda_{m-1} |c_0^{(m-1)}|^2 \right\}, \\ &\vdots \end{aligned} \quad (10)$$

Note that, if the order of the matrix $A(t)$ is an even number, $c_0^{(0)}$ equals zero. As the order of the matrix $A(t)$ increases, it is impossible to get the analytical expression of λ_k and the expression of the coefficient C_k becomes more complex. However, the phase of the coefficient C_k can be found from Eq. (10). The arguments of the coefficients are given by

$$\begin{aligned} \arg(C_0) &= 0 + (\pi), \\ \arg(C_1) &= \pi/2 - \arg(\beta_{10}) + (\pi), \\ \arg(C_2) &= -\arg(\beta_{10}) - \arg(\beta_{21}) + (\pi), \\ \arg(C_3) &= \pi/2 - \arg(\beta_{10}) - \arg(\beta_{21}) - \arg(\beta_{32}) + (\pi), \\ \arg(C_4) &= -\arg(\beta_{10}) - \arg(\beta_{21}) - \arg(\beta_{32}) - \arg(\beta_{43}) + (\pi), \\ &\vdots \end{aligned} \quad (11)$$

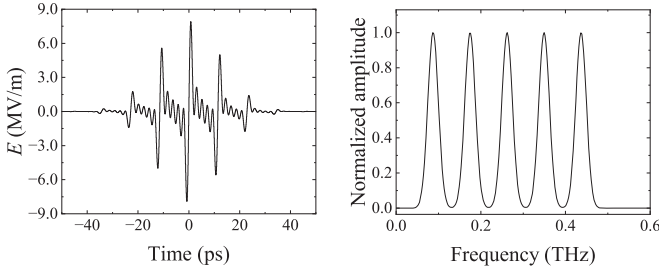


FIG. 1. The temporal shape and the frequency spectrum for the scheme involving five resonant laser pulses with $\tau = 30$ ps and electric-field amplitude 2 MV/m. The carrier-envelope phases of the laser pulses ϕ_J are set to $-\pi/2$.

The notation (π) in Eq. (11) means that sometimes we have to add π to the value of $\arg(C_k)$. This is related to the value in the curly bracket in Eq. (10), which is a real number. If the value in the curly bracket is a positive number, we do not have to add π to the value of $\arg(C_k)$, while if it is a negative number, we have to add π to the value of $\arg(C_k)$. The value in the curly bracket is related to $\beta_{k,k-1}$ and λ_k which are determined by the parameters specifying the peak amplitude and duration of the laser pulses.

According to Eq. (11), the constant phase differences between adjacent rotational states are given by

$$\begin{aligned}\varphi_{1,0} &= -\arg(\beta_{10}) + \pi/2 + (\pi), \\ \varphi_{2,1} &= -\arg(\beta_{21}) - \pi/2 + (\pi), \\ \varphi_{3,2} &= -\arg(\beta_{32}) + \pi/2 + (\pi), \\ \varphi_{4,3} &= -\arg(\beta_{43}) - \pi/2 + (\pi), \\ &\vdots \\ \varphi_{J,J-1} &= -\arg(\beta_{J,J-1}) + (-1)^{J-1}\pi/2 + (\pi),\end{aligned}\quad (12)$$

where $\beta_{J,J-1}$ at $t = t_f$ (t_f is the time after the pulses have vanished) is defined in Eq. (6), which is the product of the transition-dipole moment $\mu_{J,J-1}$ and Fourier transform of the electric field at $\omega_{J,J-1}$. For the Gaussian pulse in Eq. (1), $\arg(\beta_{J,J-1}) = \phi_J + \omega_{J,J-1}t_J$ and $\arg(\beta_{J,J-1}) = \phi_J$ when $\omega_{J,J-1}t_J = 2k\pi$ ($k = 0, \pm 1, \pm 2, \dots$). We can set $\arg(\beta_{1,0})$ to any value and the other values of $\arg(\beta_{J,J-1})$ ($J \neq 1$) can be solved according to Eq. (12) and the phase

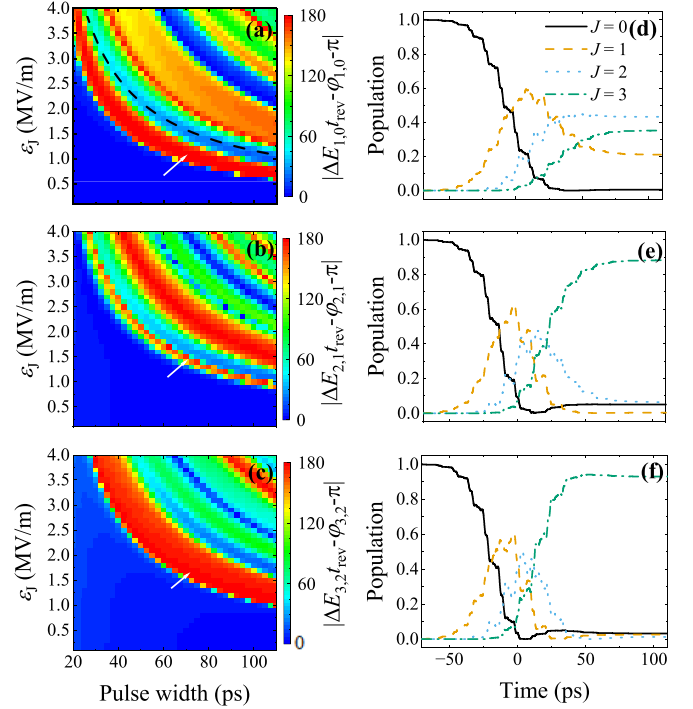


FIG. 3. The difference between $\Delta E_{J,J-1}t - \phi_{J,J-1}$ and π at full revival times for (a) $J = 1$, (b) $J = 2$, and (c) $J = 3$ in the three-pulse scheme as a function of peak amplitude and pulse width with $\phi_J = -\pi/2$. The right panels show the evolution of the rotation population with time and the laser parameters (d) $\varepsilon_J = 1.0 \times 10^6$ V/m and $\tau = 70$ ps, (e) $\varepsilon_J = 1.4 \times 10^6$ V/m and $\tau = 70$ ps, and (f) $\varepsilon_J = 1.6 \times 10^6$ V/m and $\tau = 70$ ps corresponding to the position of the arrow in panels (a)–(c).

conditions in Eq. (3). We choose $\arg(\beta_{J,J-1})$ to be equal to the same value for all J , considering the phase conditions in Eq. (3) and neglecting (π) in Eq. (12), and we get $\arg(\beta_{J,J-1})$ equals to $-\pi/2$ or $\pi/2$.

As a result, we have a simple solution for the case $\omega_{J,J-1}t_J = 2k\pi$, the phase conditions can be satisfied by choosing the carrier-envelope phase ϕ_J equal to either $-\pi/2$ or $\pi/2$. As the peak amplitude or the duration of the pulse changes gradually, the sign in the curly brackets in Eq. (10) will suddenly change at a certain laser parameter, which results in a sudden change of $\varphi_{J,J-1}$ by π , i.e., $\varphi_{1,0}$ changes from

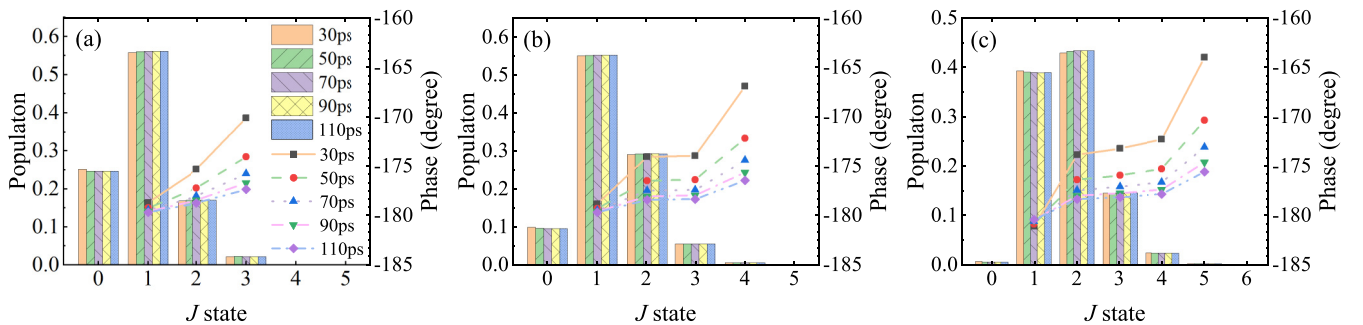


FIG. 2. Field-free population of the rotational states and the phase difference $\Delta E_{J,J-1}t - \phi_{J,J-1}$ at full revival times as a function of J for (a) three, (b) four, and (c) five pulses with $\tau = 30, 50, 70, 90$, and 110 ps and identical peak times. The carrier-envelope phase ϕ_J is set to $-\pi/2$.

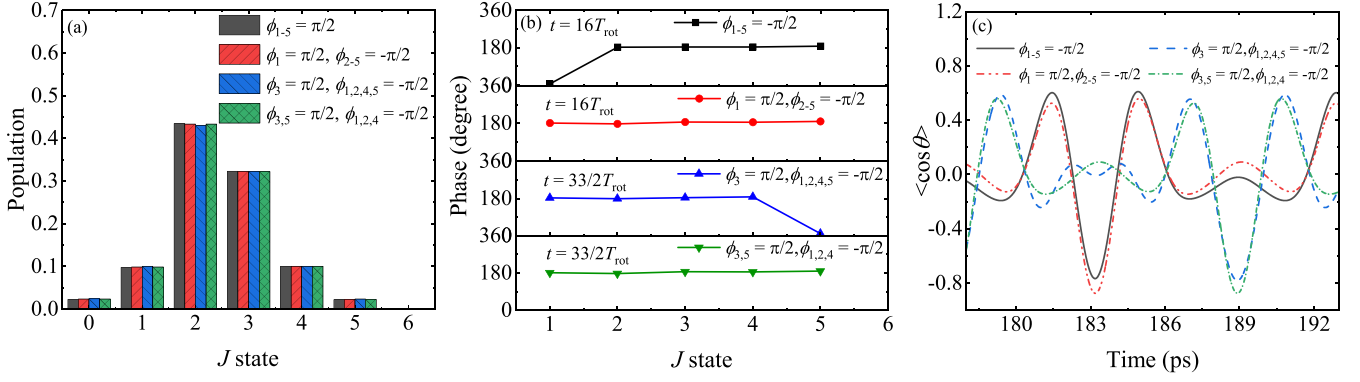


FIG. 4. (a) The population distribution of rotational states with different carrier-envelope phases ϕ_J of five laser pulses. (b) The phase difference $\Delta E_{J,J-1}t - \phi_{J,J-1}$ at full revival times as a function of J for different combinations of carrier-envelope phases of the laser pulses. (c) Orientation dynamics with respect to the combination of carrier-envelope phases of the laser pulses. The laser parameters are $\varepsilon_J = 1.1 \times 10^6$ V/m and $\tau = 70$ ps.

$-\arg(\beta_{10}) + \pi/2$ to $-\arg(\beta_{10}) + \pi/2 + \pi$. If the phase condition is destroyed, we can just change the carrier-envelope phase ϕ_1 by π to satisfy the phase condition.

III. RESULTS AND DISCUSSION

The linear molecule HCN is selected as a model. The parameters of the molecule used in our calculation are as

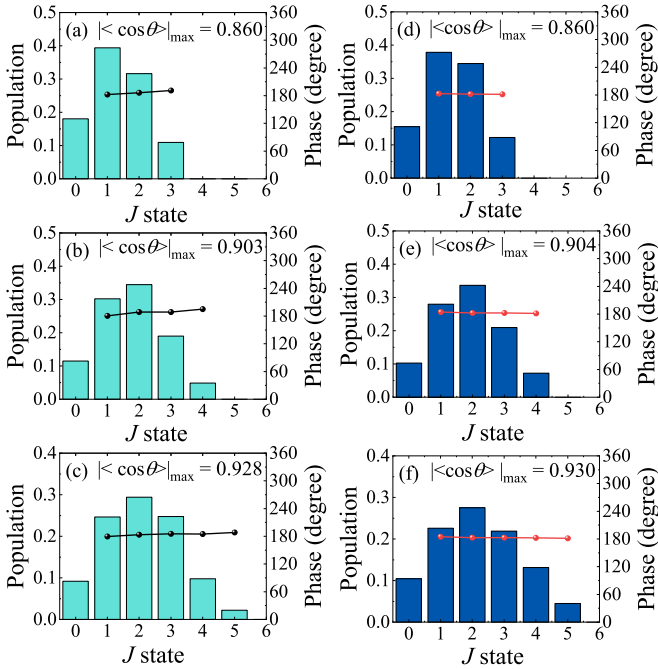


FIG. 5. The population distribution and phase difference $\Delta E_{J,J-1}t - \phi_{J,J-1}$ at full revival times as a function of J . The pulse width of each pulse is 30 ps. ϕ_J is set to $-\pi/2$. (a)–(c) show the results for laser pulses for the case $t_J = 0$, and (d)–(f) show the results for time-delayed laser pulses with center time $t_J = 2(J-1)T_{\text{rot}}$. The peak amplitude of each laser pulse, with a unit of 10^6 V/m, is shown as follows: (a) $\varepsilon_1 = 1.5$, $\varepsilon_2 = 2.0$ and $\varepsilon_3 = 1.9$; (b) $\varepsilon_1 = 1.7$, $\varepsilon_2 = 2.4$, $\varepsilon_3 = 2.5$ and $\varepsilon_4 = 2.2$; (c) $\varepsilon_1 = 1.8$, $\varepsilon_2 = 2.7$, $\varepsilon_3 = 3.1$, $\varepsilon_4 = 2.9$ and $\varepsilon_5 = 2.6$; (d) $\varepsilon_1 = 1.4$, $\varepsilon_2 = 1.2$ and $\varepsilon_3 = 0.8$; (e) $\varepsilon_1 = 1.5$, $\varepsilon_2 = 1.4$, $\varepsilon_3 = 1.1$ and $\varepsilon_4 = 0.8$; (f) $\varepsilon_1 = 1.5$, $\varepsilon_2 = 1.5$, $\varepsilon_3 = 1.3$, $\varepsilon_4 = 1.1$ and $\varepsilon_5 = 0.8$.

follows [33]: $B = 1.457$ cm $^{-1}$ and $\mu = 2.89$ D. The fundamental energy difference ($2B$) corresponds to 0.0874 THz. The molecular model is considered at $T = 0$ K. At first, we set the delay times between the laser pulses to zero, i.e., $t_J = 0$ for all J . According to the derivation in Sec. II B, to satisfy the phase condition, the carrier-envelope phases of the laser pulses ϕ_J are set to $-\pi/2$. The peak amplitude ε_J of each pulse is set to the same value. In order that there is no overlap between the frequency spectrum of each laser pulse, we have to set the pulse width larger than 30 ps. The resonant frequencies $\omega_{J,J-1}$ of the laser pulses are ($2B$, $4B$, $6B$) for the three-pulse scheme and ($2B$, $4B$, $6B$, $8B$, $10B$) for the five-pulse scheme. The temporal shape and the frequency spectrum for five resonant laser pulses with $\tau = 30$ ps are shown in Fig. 1. The populations and phase differences $\Delta E_{J,J-1}t - \phi_{J,J-1}$ at full revival times after three, four, and five laser pulses are shown in Fig. 2. As the pulse width increases, a nearly identical phase difference of π is obtained, which matches the analytic derivation in Sec. II B. It has been explained in Ref. [42] that a pulse with narrow bandwidth is beneficial for suppressing optical transitions via the higher-order terms in the Magnus expansion. That is, the validity of the analytical analysis is best in the narrow-bandwidth regime.

It should be noted that, as the pulse width is changed in Fig. 2, the absolute value of the pulse area is kept constant (i.e., $\int_{-\infty}^{\infty} |E(t)|dt = C$). Then a nearly identical population distribution is obtained after the laser pulses, see also Ref. [44]. As the absolute area of the pulses is a key parameter for the dynamics of the system, we further investigate the dependence of the phase difference on the absolute area of the pulses.

Figures 3(a)–3(c) shows the difference between $\Delta E_{J,J-1}t - \phi_{J,J-1}$ and π at full revival times for the three-pulse scheme with different peak amplitudes ε_J and pulse durations τ . For Gaussian pulses, we find that the absolute area of the pulses is proportional to the value $\varepsilon_J\tau$. The relationship between ε_J and τ and the absolute area of the pulses give a curve which is a hyperbola in Figs. 3(a)–3(c). The value of $\Delta E_{J,J-1}t - \phi_{J,J-1}$ on the same hyperbolic curve varies as the pulse duration increases. This variation decreases as the pulse width increases [see the dashed line in Fig. 3(a)].

The same result can be found in Fig. 2. It is found that the phase condition can be well satisfied when the absolute area of the pulses is less than a certain value (the blue region in the lower left corner of the figures). As the absolute area of the pulses increase, which means the hyperbolic curve will move away from the origin in Figs. 3(a)–3(c), $\Delta E_{1,0}t - \varphi_{1,0}$ suddenly changes from π to zero at the boundary between the blue and red regions [Fig. 3(a)]. Then $\Delta E_{2,1}t - \varphi_{2,1}$ and $\Delta E_{3,2}t - \varphi_{3,2}$ suddenly changes successively as the absolute area of the pulses further increase [Fig. 3(b) and 3(c)]. As discussed in Sec. II B, the sign of the value in the curly brackets in Eq. (10) is dependent on the peak amplitude and duration of the laser pulses. As the sign changes, a sudden change of $\varphi_{J,J-1}$ will be observed resulting in the sudden change of $\Delta E_{J,J-1}t - \varphi_{J,J-1}$. The sudden change of $\varphi_{J,J-1}$ is more obvious for the laser pulses with a larger τ , which also indicates that the numerical results match better with the analytical results in the narrow-bandwidth regime. As the absolute area of the pulses is further increased, there is no sudden change of phase difference from π to zero and the optimal phase difference cannot be obtained. It indicates that, as the energy of the laser pulses is large enough, an analytic solution based on the first-order Magnus expansion cannot well describe the dynamics of the system. Therefore, we have to keep the absolute area of the pulses in the blue region in the lower left corner of Figs. 3(a)–3(c) to satisfy the phase condition in our scheme.

Figures 3(d)–3(f) show the time evolution of the populations of the rotational states when the sudden change of $\varphi_{J,J-1}$ occurs. As $\varphi_{1,0}$ suddenly changes from π to zero, the population of $J = 0$ is almost empty [see the solid line in Fig. 3(d)]. Likewise, as the amplitude of the laser pulse further increases, the sudden change of $\varphi_{2,1}$ and $\varphi_{3,2}$ occurs successively when the population of $J = 1$ and $J = 2$ approach zero, respectively [see the dashed line in Fig. 3(e) and the dotted line in Fig. 3(f)]. Considering that the value in the curly brackets in Eq. (10) changes continuously with the peak amplitude and duration of the laser pulses, $\arg(C_k)$ suddenly changes when $C_k = 0$, namely, when the population of the k th rotational state is empty. This results in the sudden change of $\varphi_{k+1,k}$. It indicates that one way to satisfy the phase condition is to control the rotational population. For example, we can control the intensity of the fundamental frequency (2B) pulse to avoid the population of $J = 0$ decaying to zero. We can also control the intensities of the other pulses to avoid the populations of the other rotational states decaying to zero.

Figure 4 shows the case where $\varphi_{1,0}$ suddenly changes from π to zero with $\varepsilon_J = 1.1 \times 10^6$ V/m and $\tau = 70$ ps for five laser pulses. According to Eq. (12), it means $\varphi_{1,0} = -\arg(\beta_{10}) + \pi/2 + \pi = -(-\pi/2) + \pi/2 + \pi = 2\pi$. We can just change the carrier-envelope phase of the first laser pulse ϕ_1 from $-\pi/2$ to $\pi/2$, resulting in $\varphi_{1,0} = \varphi_{2,1} = \varphi_{3,2} = \varphi_{4,3} = \varphi_{5,4} = \pi$. Then an optimal phase difference is obtained [the second row in Fig. 4(b)] at full revival times $t_{\text{rev}} = nT_{\text{rot}}$ ($T_{\text{rot}} = \pi/B$, $n = 1, 2, 3, \dots$). This corresponds to the negative peak around 183 ps in Fig. 4(c). We can also change the carrier-envelope phase of the other pulses to satisfy the phase condition. As shown in the third and last row in Fig. 4(b), ϕ_3 and ϕ_5 are changed from $-\pi/2$ to $\pi/2$,

successively. Then $\varphi_{3,2}$ and $\varphi_{5,4}$ change from π to zero and the phase condition is satisfied as well ($\varphi_{1,0} = \varphi_{3,2} = \varphi_{5,4} = 2\pi$, $\varphi_{2,1} = \varphi_{4,3} = \pi$). It can be seen that the full revival time does not occur at the time, which is an integer multiple of the rotational period. However, the phase difference $\Delta E_{J,J-1}t - \varphi_{J,J-1}$ equals $(2k+1)\pi$ ($k = 0, \pm 1, \pm 2, \dots$) at $t_{\text{rev}} = nT_{\text{rot}} + T_{\text{rot}}/2$ ($n = 1, 2, 3, \dots$). Consequently, the full revival time is delayed by half a rotational period [see the negative peak around 189 ps in Fig. 4(c)]. Interestingly, as the carrier-envelope phases are modified, the rotational populations are unchanged [Fig. 4(a)]. Equation (10) shows that the populations of rotational states, namely $|C_k|^2$, are independent of the carrier-envelope phases ϕ_J .

The maximum values of $|\langle \cos\theta \rangle|_{\text{max}}$ for $J_{\text{max}} = 3, 4$, and 5 are 0.861, 0.906, and 0.932, respectively [22]. To get the optimal degree of orientation, we keep the phase condition to be satisfied and modify the peak amplitude of each laser pulse with a specific FWHM. To avoid a sudden change of $\varphi_{J,J-1}$, the peak amplitude of the fundamental frequency pulse is controlled to avoid the population of $J = 0$ decaying to 0. As shown in Fig. 5, where three pulses [Fig. 5(a)], four pulses [Fig. 5(b)], and five pulses [Fig. 5(c)] are utilized to control the rotational state population, the maximum degree of orientation reaches 0.860, 0.903, and 0.928, respectively, which is very close to the optimal values. Keeping the absolute area of the pulses constant, as the pulse duration increases, a flatter phase difference can be obtained at full revival times, which is beneficial for getting a higher degree of orientation.

Finally, we investigate the scheme by considering time-delayed laser pulses. To satisfy the phase condition, the center time of the laser pulses must satisfy $\omega_{J,J-1}t_J = 2k\pi$ ($k = 1, 2, 3, \dots$). Figures 5(d)–5(f) show the rotational population and phase difference at full revival times after the laser pulses have decayed. The optimal degree of orientation can be obtained again. Furthermore, the peak amplitudes of the time-delayed laser pulses are lower than those of the zero-delayed pulses. It provides a method to get the optimal degree of orientation utilizing resonant laser pulses with less energy based on our scheme.

IV. CONCLUSION AND OUTLOOK

We have used a set of resonant laser pulses to control the molecular orientation of HCN. An analytical result for multilevel systems ($J > 2$) is derived based on the first-order Magnus expansion. According to the analytical result, we can modify the carrier-envelope phase of the laser pulses to satisfy a phase condition, such that an optimal phase difference between rotational states can be obtained at full revival times. When the absolute area of the laser pulses is kept constant, below a certain threshold, the rotational population distribution after the pulses, which is independent of the carrier-envelope phases, remains unchanged. The dependence of the phase difference $\Delta E_{J,J-1}t - \varphi_{J,J-1}$ on the absolute area of the pulses is discussed and the sudden change of $\varphi_{J,J-1}$ can be well explained based on our analytical model. However, the analytical model cannot describe the dynamics of the system for laser pulses with high energy. According to the evolution of the populations of rotational states, we find a method to avoid the sudden change of $\varphi_{J,J-1}$. Thus, by adjusting the

peak amplitude below a certain value, the rotational populations can be selectively changed without changing the phase condition.

The optimal degrees of orientation for 4, 5, and 6 populated rotational states are obtained by modifying the peak amplitudes of the laser pulses. Furthermore, we find that the optimal degree of orientation can be obtained by time-delayed laser pulses with smaller peak amplitudes. The present scheme is applicable beyond the example of HCN. We note that the pulse amplitudes described here $\approx 10^6$ V/m with durations of 30 ps and up to 110 ps may be hard to achieve by the commonly used THz generation techniques. For molecules with larger

moments of inertia, the resonant transitions move into the microwave region. As the validity of our analytical analysis is best in the narrow-bandwidth regime, the method will work even better for nanosecond pulses. Tailored nanosecond pulses of the type used in the present work are now available in the microwave region [45].

ACKNOWLEDGMENTS

This work was supported by the Natural Science Foundation of Liaoning Province of China (Grant No. 2019-ZD-0009).

- [1] I. V. Litvinyuk, K. F. Lee, P. W. Dooley, D. M. Rayner, D. M. Villeneuve, and P. B. Corkum, Alignment-Dependent Strong Field Ionization of Molecules, *Phys. Rev. Lett.* **90**, 233003 (2003).
- [2] S. Petretti, Y. V. Vane, A. Saenz, A. Castro, and P. Decleva, Alignment-Dependent Ionization of N₂, O₂, and CO₂ in Intense Laser Fields, *Phys. Rev. Lett.* **104**, 223001 (2010).
- [3] H. Li, D. Ray, S. De, I. Znakovskaya, W. Cao, G. Laurent, Z. Wang, M. F. Kling, A.-T. Le, and C. L. Cocke, Orientation dependence of the ionization of CO and NO in an intense femtosecond two-color laser field, *Phys. Rev. A* **84**, 043429 (2011).
- [4] M. Kling, C. Siedschlag, A. J. Verhoef, J. Khan, M. Schultze, T. Uphues, Y. Ni, M. Uiberacker, M. Drescher, F. Krausz *et al.*, Control of electron localization in molecular dissociation, *Science* **312**, 246 (2006).
- [5] V. Aquilanti, M. Bartolomei, F. Pirani, D. Cappelletti, F. Vecchiocattivi, Y. Shimizu, and T. Kasai, Orienting and aligning molecules for stereochemistry and photodynamics, *Phys. Chem. Chem. Phys.* **7**, 291 (2005).
- [6] M. Lemesko, R. V. Krems, J. M. Doyle, and S. Kais, Manipulation of molecules with electromagnetic fields, *Mol. Phys.* **111**, 1648 (2013).
- [7] K. Lin, I. Tutunnikov, J. Ma, J. Qiang, L. Zhou, O. Faucher, Y. Prior, I. S. Averbukh, and J. Wu, Spatiotemporal rotational dynamics of laser-driven molecules, *Adv. Photonics* **2**, 024002 (2020).
- [8] T. Kanai, S. Minemoto, and H. Sakai, Quantum interference during high-order harmonic generation from aligned molecules, *Nature (London)* **435**, 470 (2005).
- [9] K.-J. Yuan and A. D. Bandrauk, Symmetry in circularly polarized molecular high-order harmonic generation with intense bicircular laser pulses, *Phys. Rev. A* **97**, 023408 (2018).
- [10] C.-T. Le, V.-H. Hoang, L.-P. Tran, and V.-H. Le, Effect of the dynamic core-electron polarization of CO molecules on high-order harmonic generation, *Phys. Rev. A* **97**, 043405 (2018).
- [11] J. Itatani, J. Levesque, D. Zeidler, H. Niikura, H. Pépin, J.-C. Kieffer, P. B. Corkum, and D. M. Villeneuve, Tomographic imaging of molecular orbitals, *Nature (London)* **432**, 867 (2004).
- [12] X.-B. Bian and A. D. Bandrauk, Probing Nuclear Motion by Frequency Modulation of Molecular High-Order Harmonic Generation, *Phys. Rev. Lett.* **113**, 193901 (2014).
- [13] W. Boutu, S. Haessler, H. Merdji, P. Breger, G. Waters, M. Stankiewicz, L. Frasninski, R. Taieb, J. Caillat, A. Maquet *et al.*, Coherent control of attosecond emission from aligned molecules, *Nat. Phys.* **4**, 545 (2008).
- [14] S. Trippel, T. Mullins, N. L. M. Müller, J. S. Kienitz, J. J. Omiste, H. Stapelfeldt, R. González-Férez, and J. Küpper, Strongly driven quantum pendulum of the carbonyl sulfide molecule, *Phys. Rev. A* **89**, 051401(R) (2014).
- [15] I. S. Averbukh and R. Arvieu, Angular Focusing, Squeezing, and Rainbow Formation in a Strongly Driven Quantum Rotor, *Phys. Rev. Lett.* **87**, 163601 (2001).
- [16] L. Coudert, Optimal control of the orientation and alignment of an asymmetric-top molecule with terahertz and laser pulses, *J. Chem. Phys.* **148**, 094306 (2018).
- [17] C. P. Koch, M. Lemesko, and D. Sugny, Quantum control of molecular rotation, *Rev. Mod. Phys.* **91**, 035005 (2019).
- [18] Y. Sugawara, A. Goban, S. Minemoto, and H. Sakai, Laser-field-free molecular orientation with combined electrostatic and rapidly-turned-off laser fields, *Phys. Rev. A* **77**, 031403(R) (2008).
- [19] M. Muramatsu, M. Hita, S. Minemoto, and H. Sakai, Field-free molecular orientation by an intense nonresonant two-color laser field with a slow turn on and rapid turn off, *Phys. Rev. A* **79**, 011403(R) (2009).
- [20] K. Oda, M. Hita, S. Minemoto, and H. Sakai, All-Optical Molecular Orientation, *Phys. Rev. Lett.* **104**, 213901 (2010).
- [21] J. J. Omiste and R. González-Férez, Rotational dynamics of an asymmetric-top molecule in parallel electric and nonresonant laser fields, *Phys. Rev. A* **88**, 033416 (2013).
- [22] S. Wang and N. E. Henriksen, Optimal field-free molecular orientation with nonresonant two-color adiabatic-turn-on and sudden-turn-off laser pulses, *Phys. Rev. A* **102**, 063120 (2020).
- [23] T. Kanai and H. Sakai, Numerical simulations of molecular orientation using strong, nonresonant, two-color laser fields, *J. Chem. Phys.* **115**, 5492 (2001).
- [24] R. Tehini and D. Sugny, Field-free molecular orientation by nonresonant and quasiresonant two-color laser pulses, *Phys. Rev. A* **77**, 023407 (2008).
- [25] J. Wu and H. Zeng, Field-free molecular orientation control by two ultrashort dual-color laser pulses, *Phys. Rev. A* **81**, 053401 (2010).
- [26] K. Lin, I. Tutunnikov, J. Qiang, J. Ma, Q. Song, Q. Ji, W. Zhang, H. Li, F. Sun, X. Gong, *et al.*, All-optical field-free three-dimensional orientation of asymmetric-top molecules, *Nat. Commun.* **9**, 5134 (2018).

- [27] C.-C. Shu, K.-J. Yuan, W.-H. Hu, and S.-L. Cong, Field-free molecular orientation with terahertz few-cycle pulses, *J. Chem. Phys.* **132**, 244311 (2010).
- [28] C. Qin, Y. Tang, Y. Wang, and B. Zhang, Field-free orientation of CO by a terahertz few-cycle pulse, *Phys. Rev. A* **85**, 053415 (2012).
- [29] N. E. Henriksen, Molecular alignment and orientation in short pulse laser fields, *Chem. Phys. Lett.* **312**, 196 (1999).
- [30] C. Dion, A. Keller, and O. Atabek, Orienting molecules using half-cycle pulses, *Eur. Phys. J. D* **14**, 249 (2001).
- [31] M. Machholm and N. E. Henriksen, Field-Free Orientation of Molecules, *Phys. Rev. Lett.* **87**, 193001 (2001).
- [32] D. Sugny, A. Keller, O. Atabek, D. Daems, S. Guérin, and H. R. Jauslin, Time-dependent unitary perturbation theory for intense laser-driven molecular orientation, *Phys. Rev. A* **69**, 043407 (2004).
- [33] C.-C. Shu, Q.-Q. Hong, Y. Guo, and N. E. Henriksen, Orientational quantum revivals induced by a single-cycle terahertz pulse, *Phys. Rev. A* **102**, 063124 (2020).
- [34] K. Kitano, N. Ishii, N. Kanda, Y. Matsumoto, T. Kanai, M. Kuwata-Gonokami, and J. Itatani, Orientation of jet-cooled polar molecules with an intense single-cycle THz pulse, *Phys. Rev. A* **88**, 061405(R) (2013).
- [35] Z.-Y. Zhao, Y.-C. Han, Y. Huang, and S.-L. Cong, Field-free orientation by a single-cycle THz pulse: The NaI and IBr molecules, *J. Chem. Phys.* **139**, 044305 (2013).
- [36] K. Kitano, N. Ishii, and J. Itatani, High degree of molecular orientation by a combination of THz and femtosecond laser pulses, *Phys. Rev. A* **84**, 053408 (2011).
- [37] H. Li, W. Li, Y. Feng, H. Pan, and H. Zeng, Field-free molecular orientation by femtosecond dual-color and single-cycle THz fields, *Phys. Rev. A* **88**, 013424 (2013).
- [38] C.-C. Shu and N. E. Henriksen, Field-free molecular orientation induced by single-cycle THz pulses: The role of resonance and quantum interference, *Phys. Rev. A* **87**, 013408 (2013).
- [39] H. Yun, H. T. Kim, C. M. Kim, C. H. Nam, and J. Lee, Parity-selective enhancement of field-free molecular orientation in an intense two-color laser field, *Phys. Rev. A* **84**, 065401 (2011).
- [40] A. S. Chatterley, E. T. Karamatskos, C. Schouder, L. Christiansen, A. V. Jørgensen, T. Mullins, J. Küpper, and H. Stapelfeldt, Communication: Switched wave packets with spectrally truncated chirped pulses, *J. Chem. Phys.* **148**, 221105 (2018).
- [41] E. T. Karamatskos, S. Raabe, T. Mullins, A. Trabattoni, P. Stammer, G. Goldsztejn, R. R. Johansen, K. Długołęcki, H. Stapelfeldt, M. J. Vrakking *et al.*, Molecular movie of ultrafast coherent rotational dynamics of OCS, *Nat. Commun.* **10**, 3364 (2019).
- [42] Q.-Q. Hong, L.-B. Fan, C.-C. Shu, and N. E. Henriksen, Generation of maximal three-state field-free molecular orientation with terahertz pulses, *Phys. Rev. A* **104**, 013108 (2021).
- [43] S. Ramakrishna and T. Seideman, Intense Laser Alignment in Dissipative Media as a Route to Solvent Dynamics, *Phys. Rev. Lett.* **95**, 113001 (2005).
- [44] T. K. Begzjav and H. Eleuch, Magnus expansion applied to a dissipative driven two-level system, *Results Phys.* **17**, 103098 (2020).
- [45] C. Pérez, A. L. Steber, S. R. Domingos, A. Krin, D. Schmitz, and M. Schnell, Coherent enantiomer-selective population enrichment using tailored microwave fields, *Angew. Chem., Int. Ed.* **56**, 12512 (2017).